

1 *Article*2 **Coupled electric and hydraulic control of a PRS**
3 **turbine in a real transport water network**4 **Marco Sinagra^{1,*}, Costanza Aricò¹, Tullio Tucciarelli¹, Pietro Amato² and Michele Fiorino³**5 ¹ Dipartimento di Ingegneria, Università degli Studi di Palermo, viale delle Scienze, 90128, Palermo, Italy;
6 marco.sinagra@unipa.it, costanza.arico@unipa.it, tullio.tucciarelli@unipa.it7 ² WECONS company, via Agrigento n.67, 90141, Palermo, Italy;
8 p.amato@wecons.it9 ³ Layer Electronics company, S.P. KM 5,3 C.da S. Cusumano, 91100 Erice (TP) - Italy;
10 info@layer.it

11 * Correspondence: marco.sinagra@unipa.it; Tel.: +39-091-238-96518

12

13 **Abstract:** Although many devices have recently been proposed for pressure regulation and energy
14 harvesting in water distribution and transport networks, very few applications are still
15 documented in the scientific literature. A new in-line Banki turbine with positive outflow pressure
16 and a mobile regulating flap, named PRS, was installed and tested in a real water transport
17 network for pressure and discharge regulation. The PRS turbine was directly connected to a 55 kW
18 asynchronous generator with variable rotational velocity, coupled to an inverter. The start-up tests
19 showed how automatic adjustment of the flap position and the impeller velocity variation are able
20 to change the characteristic curve of the PRS according to the flow delivered by the water manager
21 or to the pressure set-point assigned downstream or upstream of the system, still keeping good
22 efficiency values in hydropower production.

23 **Keywords:** Pressure control; Micro-hydropower; Energy recovery; Water distribution network;
24 Banki turbine; Energy harvesting

25

26 **1. Introduction**

27 Although many cities continue to use fossil fuels as their main energy source, the use of renewable
28 energy sources [1] is becoming a key political solution to mitigate climate changes occurring in the
29 world. In this context the economic and social value of water is due today not only to its domestic
30 and agricultural use, but also to the potential energy embedded in its delivery to low-altitude urban
31 areas [2,3]. Water distribution or transport networks have been traditionally designed to meet
32 consumer demands, usually variable over time, at the outlet of the pipe network, while keeping the
33 pressure within a given pressure range, to provide a high quality service level. Recently new design
34 approaches have also been based on additional hydraulic parameters such as resilience [4]. In both
35 cases, to control discharge and pressure in the water network, along the pipelines water managers
36 very often install pressure reducing valves (PRV) and needle valves. PRVs are aimed to control
37 pressure in the conduit for a given demand and needle valves are aimed to control discharge given
38 fixed outlet pressure [5,8]. An alternative to the use of valves is the use of Pumps As Turbines (PATs)
39 or small hydraulic turbines [9] to convert hydraulic energy into electricity as an alternative to
40 dissipation.

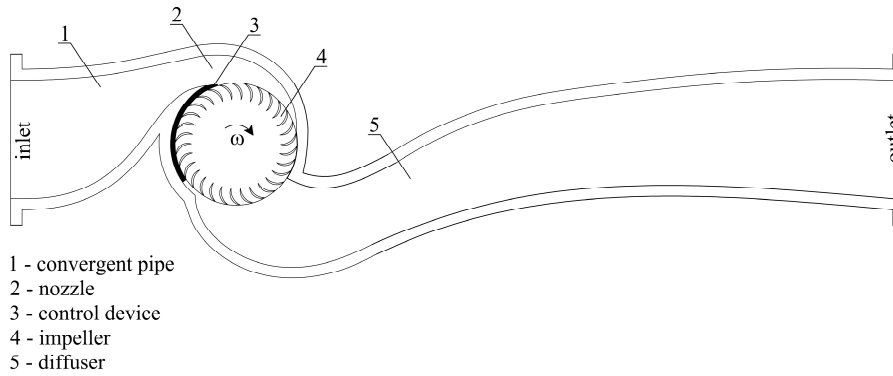
41 Nowadays many studies can be found in the literature about the use of turbines with free outlet
42 discharge [10,14] or positive outlet pressure [15]. However, the use of these turbines is limited by

43 their high cost, compared to the gross power usually available in the pipelines. For these
44 applications less expensive solutions are Crossflow mini-turbines [16] in the case of free outlet
45 discharge and PATs [17,18] in the case of positive outlet pressure. The main drawback of PATs is
46 given by the need to dissipate part of the available energy when the discharge or head jump values
47 required by the water manager are different from the design ones, due to the absence of any
48 hydraulic system to control the characteristic curve [17]. To maintain hydraulic control of the
49 network, PATs [20,21] and Crossflows [22] are often coupled with electronic systems for regulation
50 of impeller rotation velocity or with installation of PRV valves in series or parallel with the PAT [23].
51 This type of solution is also applied for the recharge of electric vehicles in urban areas [24].
52 An alternative, more efficient and also less expensive way to produce hydropower while keeping the
53 hydraulic control of the network is given by a new Crossflow-type of turbine, named PRS and
54 already proposed by the authors in previous numerical [25] and laboratory experimental studies
55 [26]. PRS has the simplicity of Crossflow turbines, but is also equipped with a hydraulic regulation
56 system which allows changes in the characteristic curve according to the specific discharge or to the
57 head jump required by the water manager. In this paper the design, the installation in a Sicilian
58 aqueduct and the start-up tests of a 55 kW PRS turbine, subject to discharge and pressure variations,
59 are described and analyzed for the first time.

60 2. PRS turbine

61 The PRS turbine is a new in-line Crossflow type micro-turbine, with positive outflow pressure and a
62 mobile regulation flap for hydraulic control of the characteristic curve, developed and tested by the
63 authors at the hydraulic laboratory of the University of Palermo [25-27].

64 A PRS turbine has five main components (Fig. Figure 1): the convergent pipe, the nozzle, the
65 mobile flap, the rotating impeller and the pressurized diffuser. The convergent pipe is aimed to
66 accelerate the particles, transforming most of the potential pressure energy into kinetic energy, and
67 the nozzle works as a/the distributor of the discharge entering the impeller through the inlet surface.
68 The mobile flap varies the inlet surface in the impeller, in order to control the velocity of the inlet
69 particle during any change in the discharge and to keep constant the ratio between the tangent
70 velocity component of the particle and the impeller rotational velocity at the same inlet location. The
71 impeller inlet and outlet surfaces are part of a cylinder, with generator lines parallel to the axis and
72 laterally bounded by the two impeller disks. The two impeller disks form a single solid block with
73 the blades, which are semi-circular and have a constant inner radius. Water flow goes through the
74 blade channels twice, before leaving the impeller and entering the diffuser section. This part, which
75 is missing in the original Crossflow turbine for zero-pressure outlet flow, is designed in order to
76 minimize dissipation of the particle-specific energy along the path between the impeller and the
77 outlet section of the turbine case. The PRS turbine can be set in the "passive" or "active" mode. In the
78 former the device is used to set the piezometric level at any required value, lower than the inlet one,
79 but even much greater than the ground elevation, while also being variable in time. In the "active"
80 mode, the device is used to set the discharge at any required value by controlling the flap position
81 and the pressure reduction occurring between the inlet and outlet pipe sections.
82



83
84 **Figure 1.** Vertical section of a PRS turbine.
85

86 Turbine design has to satisfy three conditions assigned at the Best Efficiency Point (BEP) among
87 the impeller diameter D , the rotational velocity ω , the discharge Q and the net head ΔH occurring
88 between the inlet and the outlet pipes. The first equation is the energy conservation equation, which
89 according to previous studies ([25]-[27]) is given by:
90

$$91 \quad V = C_v \sqrt{2g \left(\Delta H - \xi \frac{\omega^2 D^2}{8g} \right)} \quad (1),$$

92 where V is the velocity norm at the impeller inlet surface, $C_v = 0.98$, $\xi = 2.1$ and g is the gravitational
93 acceleration.
94

95 The second equation is the mass conservation equation, which provides:
96

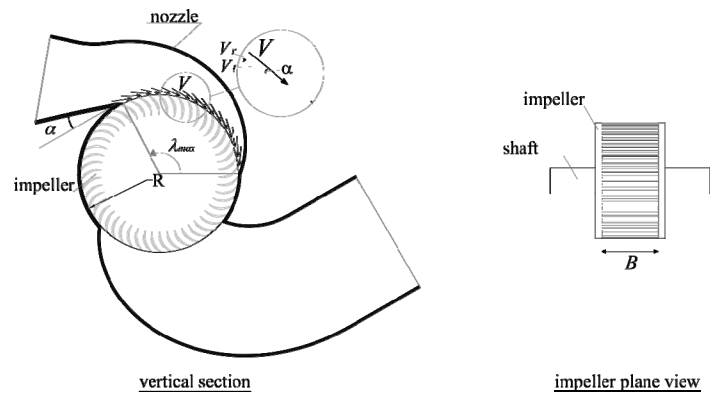
$$97 \quad Q = \frac{BD\lambda_{rmax}V \sin \alpha}{2} \quad (2),$$

98 where B is the impeller width, λ_{rmax} is the maximum inlet angle, equal to 110° , and α is the angle
99 between the particle velocity and the tangent direction at the impeller inlet (Fig. Figure 2),
100 approximately equal to 15° . The third equation is the optimality condition of the velocity ratio V_r ,
101 defined as the ratio between the tangent component of the inlet velocity and the impeller rotational
102 velocity at the same inlet surface, that is:
103

$$104 \quad V_r = \frac{DV \cos \alpha}{2\omega} \quad (3).$$

105 Sinagra et al. [25] showed that the maximum efficiency in PRS turbine is obtained assuming $V_r =$
106 1.7.

107 The diameter D and width B can be found by fixing in Eqs (1) and (3) the rotational velocity
108 ω , and by solving the system of Eqs. (1)-(3) in the unknowns V , D and B . This is the commonest
109 approach for the design of mini-hydropower turbines, where the impeller is directly connected to the shaft
110 of the asynchronous electric generator, which has a fixed rotational velocity.
111



112
113 **Figure 2.** Nozzle and impeller geometry of PRS turbine.

114 3. Electrical energy production and velocity regulation

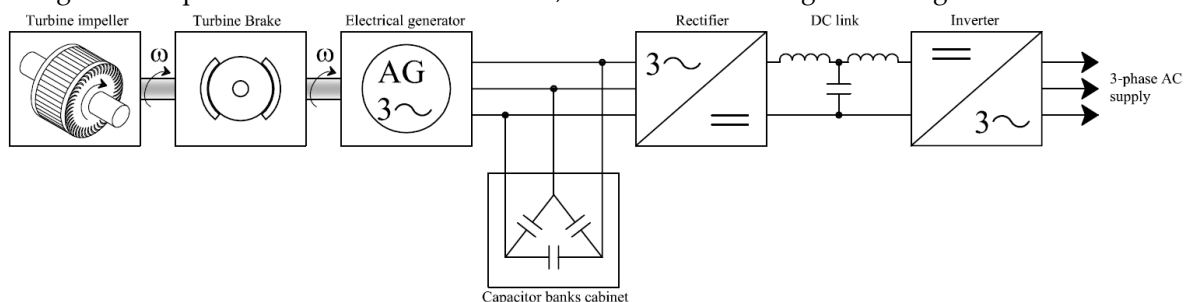
115 In small-scale hydroelectric plants, with power lower than 250 kW, the simplest way to convert
116 hydraulic power into electrical power is to couple an asynchronous three-phase generator to the
117 turbine impeller. In case (A), when the electric generator is directly connected to the AC grid, the
118 reactive power required by the electrical generator to properly operate is provided by the grid itself,
119 while in case (B), that of a stand-alone plant, the reactive power is provided by a local capacitor bank.
120 The choice of the asynchronous generator is motivated by its simplicity and robustness. However, in
121 both operation modes A and B, the rotational velocity of the electric generator is closely related to
122 the frequency f of the AC grid (grid-connected) or of the electrical equipment (stand-alone), which in
123 Europe is equal to 50 Hz, through the equation:

$$124 \quad \omega = \frac{60f}{2p} \quad (4),$$

125 where ω is the rotational velocity in rotations per minute and p is the number of poles.

126 When the net head ΔH changes along with the operating conditions of the hydraulic network,
127 equations (1) and (3) cannot be satisfied together with same diameter D , unless the impeller
128 rotational velocity ω is changed. For this reason, the rotational velocity of the impeller is optimized
129 by means of an electric system. The electric regulation system consists of a rectifier and an inverter.
130 The task of the rectifier is to convert the alternating voltage supplied by the asynchronous
131 three-phase generator, working at variable voltage and frequency, into a continuous voltage for the
132 inverter power supply. The inverter adopted is a total-control IGBT bridge in configuration B6 (three
133 branches in parallel, each one with two IGBTs in series), which commutes the continuous voltage
134 supplied by the rectifier into a sinusoidal alternating voltage at 50Hz. The reactive power required
135 by the electrical generator is provided in the stand-alone case by a local capacitor banks cabinet with
136 automatic power control (Figure 3).

137 With this configuration, the optimal rotational velocity ω of the impeller is automatically
138 attained in case B by regulating the voltage coming out of the inverter. Higher electric loads will lead
139 to higher power, but also to a reduction of the turbine rotational velocity, due to a torque resistance
140 increment. This implies that the system will shortly reach an equilibrium condition that will change,
141 along with the power delivered in the network, as a function of the given voltage.



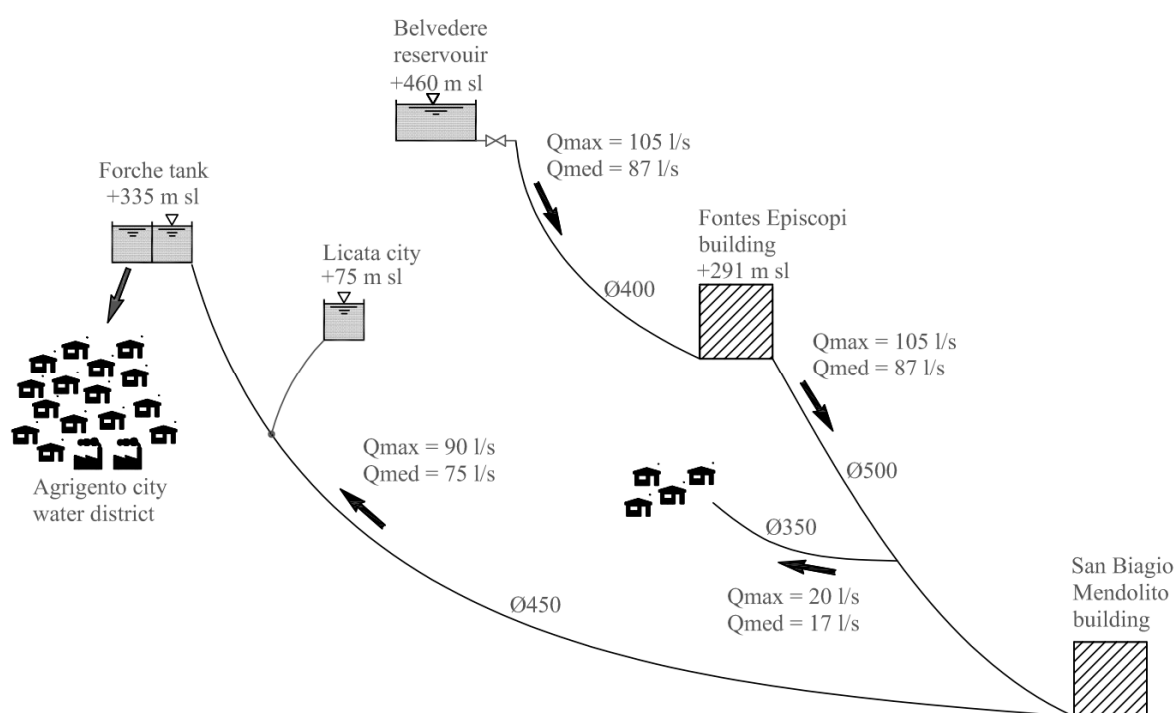
142
143 **Figure 3.** Block diagram of a direct drive power conversion unit.

144 A similar scheme can be attained in case A, by disconnecting the capacitor banks cabinet and
 145 regulating the current coming out of the inverter.

146 4. Study case: Gela-Aragona aqueduct

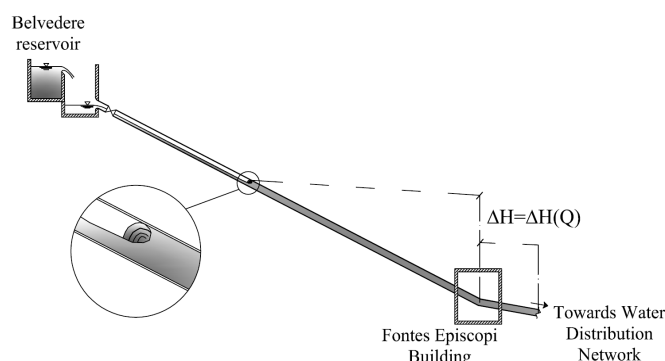
147 We investigated the design and management of a PRS turbine inline of an oversized water transport
 148 network, subject to continuous discharge regulations due to the changing demand of water users.

149 The water transport network, called the Gela-Aragona aqueduct, is part of the larger Water
 150 Transport Network of Sicily (Italy). The Gela-Ragona aqueduct starts from an upper tank, called
 151 "Belvedere" and located at an altitude of 460 m above sea level, supplying a lower tank named
 152 "Forche", located 335 m above sea level. This tank supplies the water distribution network of the city
 153 of Agrigento, as well as another tank located at an altitude of 75 m above sea level, serving the water
 154 distribution network of the town of Licata. Along the pipeline there are two pressure maneuvering
 155 buildings, called "Fontes Episcopi" and "San Biagio Mendolito", and between them there is a
 156 derivation supplying a small urban center (Fig. Figure 4). The discharge from the "Belvedere"
 157 reservoir changes in the range 70-100 l/s, and is regulated at present by a needle valve located
 158 immediately downstream of the reservoir. Inside the cited discharge range the pressure measured at
 159 the "Fontes Episcopi" building changes in the range 0.2 - 0.6 MPa. If the pressure measured at
 160 "Fontes Episcopi" is above 0.5 MPa, the "Forche" tank is filled; otherwise the flow is conveyed
 161 entirely to the Licata tank.
 162



163
 164 **Figure 4.** Scheme of the water transport network.
 165

166 Inside the cited discharge range, the pipeline connecting the "Belvedere" reservoir to the
 167 "Fontes Episcopi" building, which is 3.5 km long, is not completely full and the pressure drop ΔH of
 168 the free surface transition section inside the pipeline, with respect to the piezometric level at the
 169 "Fontes Episcopi" building, is approximately proportional to the square of the discharge released
 170 through the needle valve by the water manager (Fig. Figure 5).
 171



172
173 **Figure 5.** Hydraulic regime inside the upstream pipeline without the PRS turbine.
174

175 These operating conditions provide a hydraulic jump available for hydroelectric production
176 between the surface transition and the "Belvedere" reservoir, which can be converted into electricity
177 by a PRS turbine installed inside the Fontes Episcopi building at an altitude of 291 m above sea level.
178 The maximum electricity production would occur in the case of a fully pressurized pipe, with head
179 losses equal to 9.00 m in the case of a maximum flow rate. In order to guarantee the maximum flow
180 rate when the maximum pressure occurs at Fontes Episcopi (0.6 MPa = 60m), the following values
181 were assumed in Eqs. (1)-(3) for the design of parameters D and B in the condition of a fully opened
182 flap: $\Delta H = 100$ m and $Q = 105$ l/s.

183 Assuming a rotational velocity ω equal to 1510 rpm, the impeller diameter D and the width B
184 resulting from the procedure described in paragraph 2 are equal to 204 and 62 mm, respectively. The
185 PRS casing is made of cast iron and the impeller, made of stainless steel, has 40 semicircular blades
186 [28] connected to each other by a couple of circular plates fixed to the shaft, which rotates on two
187 bearings. There is no internal shaft. The flap is made of stainless steel and is moved by a linear
188 electrical actuator.

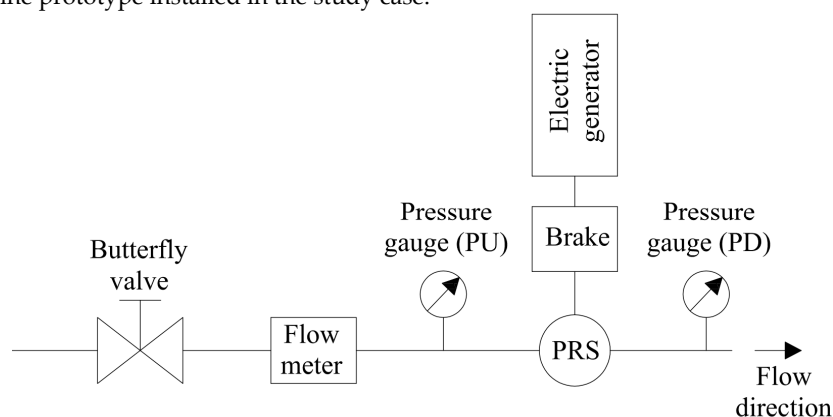
189 Small traditional hydroelectric plants are equipped with a synchronous by-pass to stop rotation
190 of the impeller in the case of failure of the electric network. This is a pipe parallel to the impeller,
191 equipped with an automatic valve, which opens to allow the entire flow to bypass the turbine when
192 electricity is missing. In the Fontes Episcopi PRS plant an alternative solution was selected. Between
193 the impeller shaft and the electric generator a negative electric-brake was installed. In the case of
194 failure of the electrical grid or an emergency, the brake is activated instantaneously to stop rotation
195 of the impeller rapidly. The total flow will continue to pass through the impeller, which will have
196 zero speed. Observe that this solution guarantees water supply even in the absence of electricity
197 production, without installing an automatic synchronous valve.

198 For electricity production, an asynchronous generator 4-pole IE2 efficiency class with 55 kW
199 power was installed. The power electronics system described in paragraph 3, with a maximum
200 electrical power of 60 kW, was connected to the electric generator. The power electronics was
201 oversized compared to the generator power to ensure system security. In Figure 6 the PRS turbine
202 prototype installed inside the Fontes Episcopi building is shown.

203 For monitoring hydraulic parameters, an electromagnetic flow meter and a digital pressure
204 meter were installed upstream of the PRS prototype and a second digital pressure meter was
205 installed downstream of the turbine to measure the net head of the turbine (Fig. Figure 7).
206



207
208 **Figure 6.** PRS turbine prototype installed in the study case.



209
210 **Figure 7.** Equipment installation scheme.

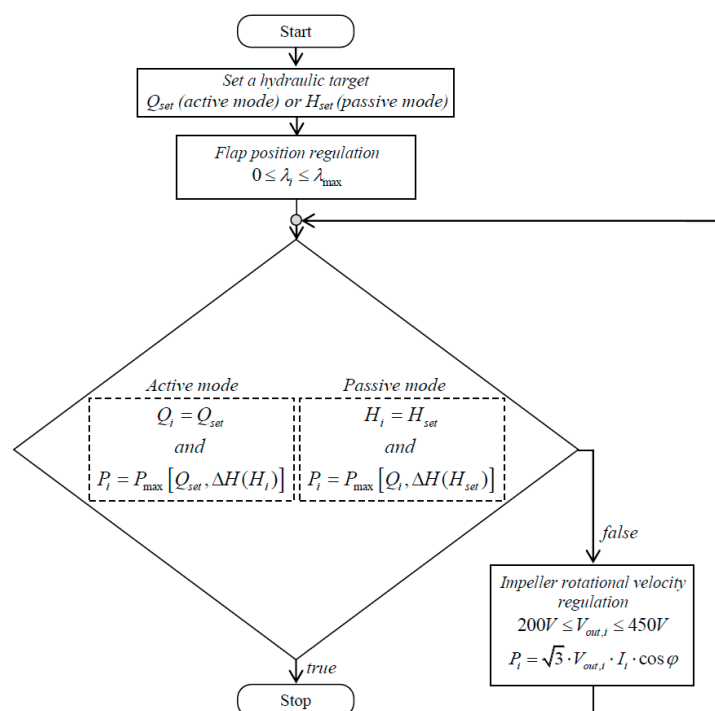
211
212 The PRS components of the pilot plant are automatically regulated by a PLC installed on the
213 electrical panel dedicated to turbine management. If the device is used in “active” mode and the
214 flow rate Q_{set} is set, the flap position is found by comparing the measure of the flow meter with its
215 target value; if the device is used in “passive” mode, the flap position is found by comparing the
216 pressure measured by the downstream or upstream pressure gauge with its pressure target value. In
217 both cases, the impeller rotational velocity is optimized by maximizing the electrical power P_i
218 coming out of the inverter, according to the Q_{set} or H_{set} values, calculated by the eq. 5:

$$219 \quad P_i = \sqrt{3} \cdot V_{out,i} \cdot I_i \cdot \cos \varphi \quad (5),$$

220 where $V_{out,i}$ and are respectively the voltage and the current coming out of the inverter and $\cos \varphi$ is
221 the power factor.

222 The control logic implemented in the PLC is represented by the flow chart in Figure 8.

223



224
225 **Figure 8.** Flow chart of PRS regulation.
226

227 The hydroelectric production performance of the plant is calculated by comparing in each time
228 the electrical output power from the inverter with the gross hydraulic power computed from the
229 flow and pressure measurements.

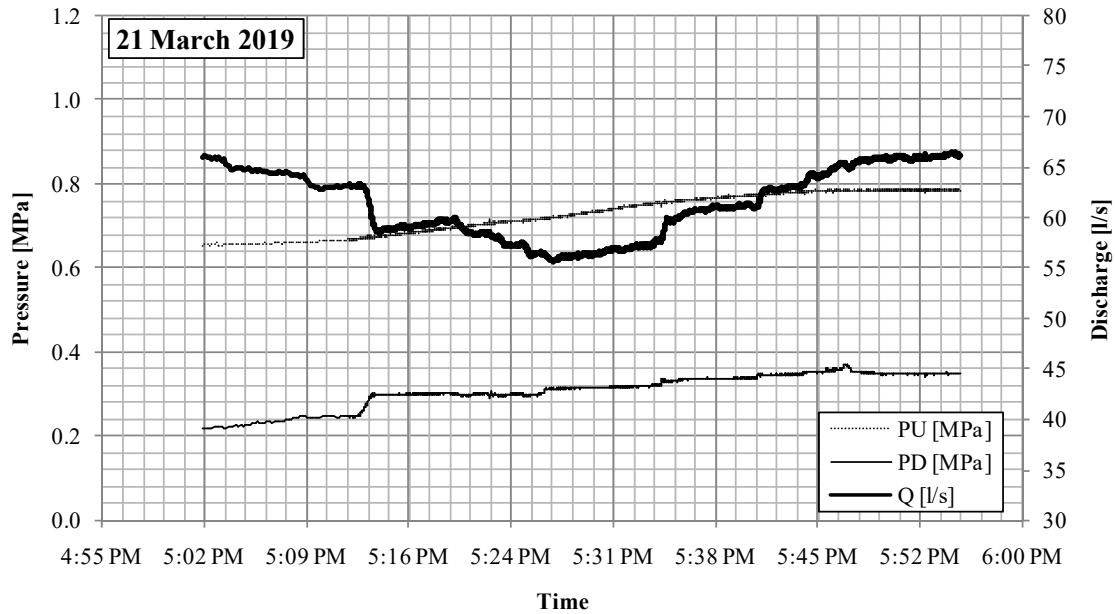
230 5. PRS turbine application results

231 During the start-up period, in order to guarantee the quality of water distribution and ensure the
232 safety of the pipeline, the water manager needs to guarantee the following operating conditions: 1) a
233 pressure in the range of 0.2-0.4 MPa downstream of the Fontes Episcopi building; 2) a pressure lower
234 than 1.0 MPa on the entire supply line; 3) discharge variable according to the given demand and in
235 any case lower than 75 l/s. Under these operation conditions, different from the turbine design
236 values, the PRS start-up tests were carried out.

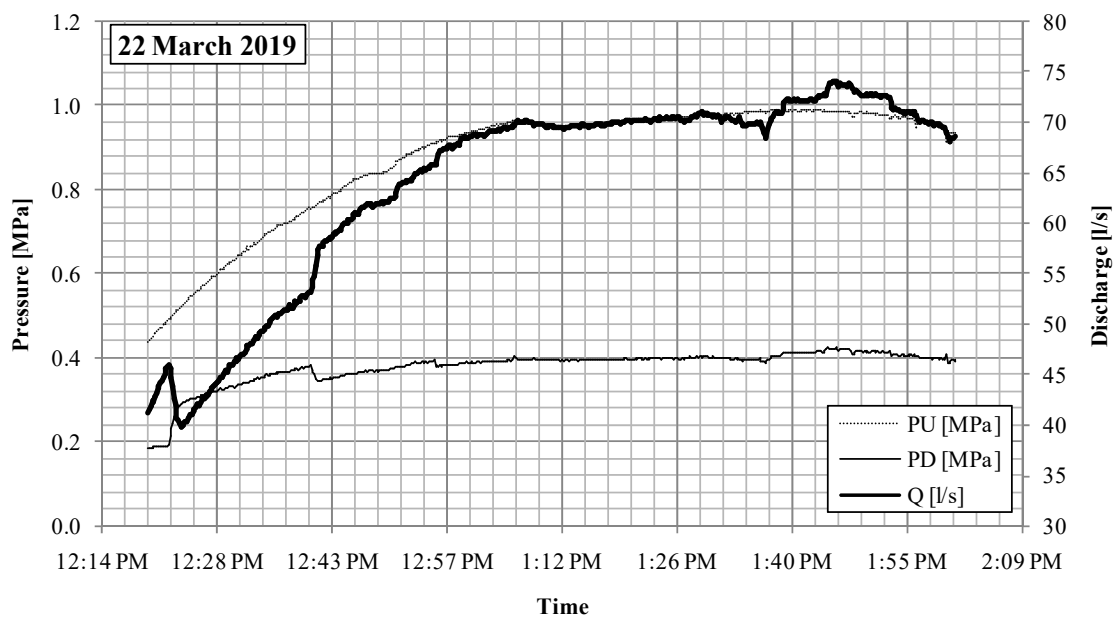
237 In the following sections, the hydraulic and power variables recorded during the start-up tests
238 on the PRS plant installed at the Fontes Episcopi building are shown. Due to the long time required
239 by bureaucracy for connection to the Italian national electric grid and electricity trading, the
240 electrical power produced by the plant during the 2 days of the start-up tests was temporarily
241 dissipated through electrical resistances.

242 During the start-up period, the device was set in passive mode, with the discharge imposed by
243 the water manager through the needle valve and shown in Figs. Figure 9 and Figure 10. Observe that,
244 with the given discharge, free surface conditions always occur inside the upper part of the pipeline.
245 The pressure immediately upstream of the PRS was set according to the manager's request, given
246 the downstream pressure curve plotted in the same figures. On the first day of testing the maximum
247 upstream pressure was set at 0.8 MPa; on the second day of testing it was set at 1.0 MPa. The time
248 series of the hydraulic data recorded during the testing period are all shown in Figs. Figure 9
249 and Figure 10.

250

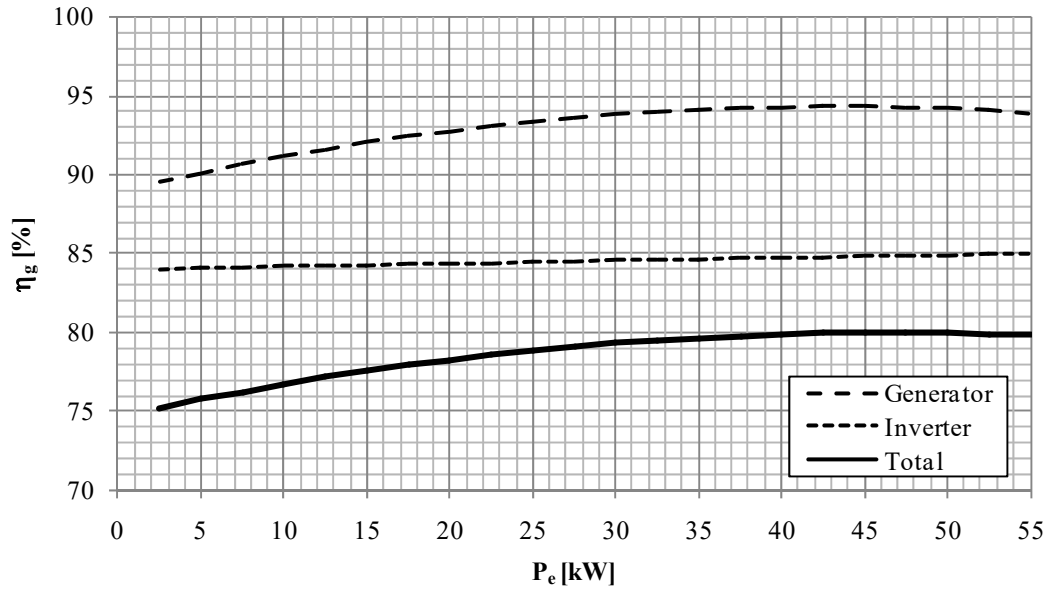


251
252 **Figure 9.** Discharge and pressure in the manometers showed in Figure 7.
253



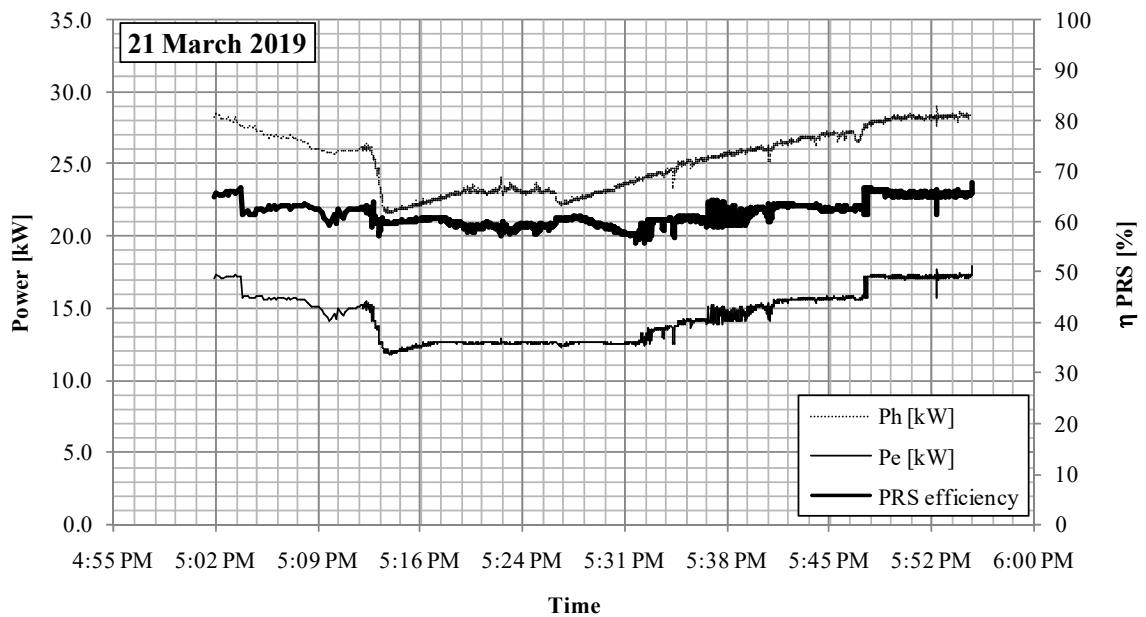
254
255 **Figure 10.** Discharge and pressure in the manometers showed in Figure 7.
256

257 In order to evaluate the global performance of the PRS and the hydroelectric plant, voltage and
258 current measurements were made at the input and output of the inverter, to get the electrical power
259 along the test time. Knowledge of the generator characteristic curve made it possible to determine
260 the efficiency of the asynchronous generator as a function of the power supplied by the generator
261 itself. The inverter's efficiency was estimated by comparing its input and the output power. The
262 electrical efficiencies are shown in Figure 11. The graph shows that the inverter has lower efficiency
263 than the electric generator, but that it is constant with respect to the supplied power.

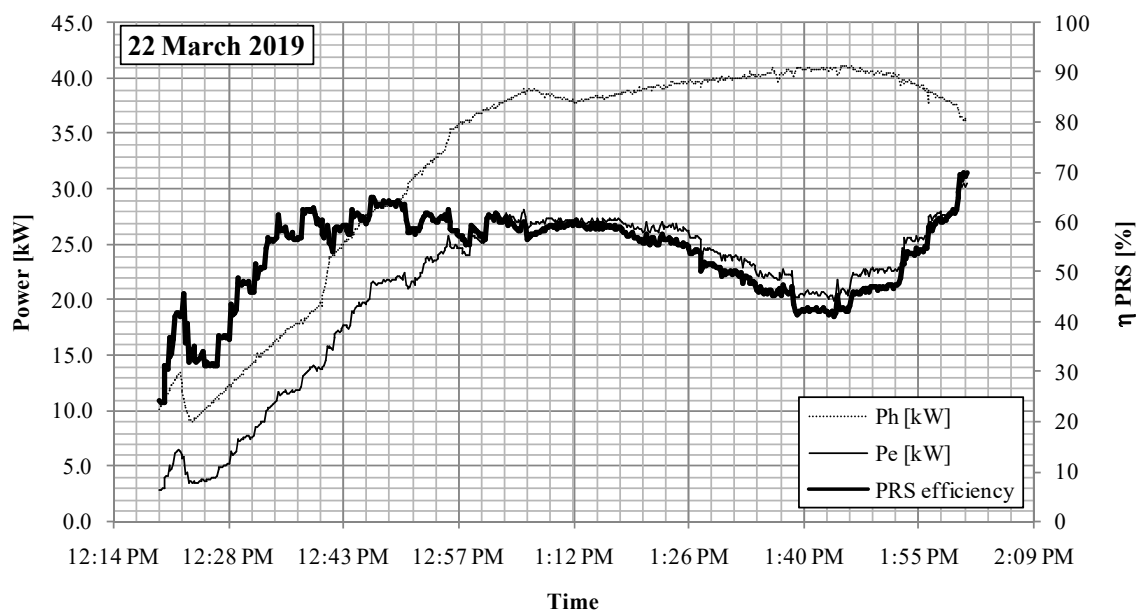


264
265 **Figure 11.** Electrical efficiencies.
266

267 The hydraulic efficiency of the PRS was computed as the ratio between the output electric power of
268 the generator and the available gross hydraulic power, multiplied by the total electrical efficiency.
269 The tests carried out show an average hydraulic efficiency of 61% on the first day and 55% on the
270 second day of operation. The hydraulic efficiency of the PRS versus time is shown in Figs. Figure 12
271 and Figure 13.



272
273 **Figure 12.** Hydraulic power, electrical power and PRS efficiency.
274



275
276 **Figure 13.** Hydraulic power, electrical power and PRS efficiency.
277

278 Some electrical disconnections of the generator were carried out during the start-up period, in
279 order to validate the effect of brake action on the water supply and on the pipeline, for different
280 discharge and pressure values. The tests confirmed the absence of overpressure in the pipeline
281 generated by the instantaneous stop of the impeller and validated the 30% increment of the
282 maximum discharge, as already numerically predicted by previous studies [25].

283 6. Conclusions

284 A new Banki-type turbine with positive outlet pressure, called PRS, was installed in a real water
285 transport network for pressure regulation. The PRS is equipped with an internal flap for discharge
286 or pressure regulation and an inverter for the impeller rotational velocity regulation. Start-up tests
287 showed that the PRS could be efficiently used in water distribution networks for regulation of flow
288 rate, as an alternative to needle valves, or for regulation of the downstream/upstream head, as an
289 alternative to PRV valves. The tests also showed that the PRS is able automatically to adjust the
290 position of its flap and optimize power production by rotational velocity regulation, according to the
291 pressure set-point required by the water manager and the instantaneous discharge. Simulation of
292 interruption of the electrical network also showed that the PRS braking system is able quickly to
293 interrupt impeller rotation, without generating overpressures on the water network. The transition
294 of the maximum flow through the stopped impeller provides a net head which is equal to the net
295 head occurring at the optimal rotating velocity divided by 1.71, as already predicted in a previous
296 study.

297 The hydraulic constraints imposed by the water manager during the start-up period did not
298 allow use of the turbine according to the design conditions, but this is unfortunately the most
299 common situation. In spite of that, the PRS mean efficiency, equal to 53% on the first testing day and
300 61% on the second testing day, coupled with a total electrical efficiency of the order of 80%, still leads
301 to a significant amount of energy and a corresponding gain for the water manager. The cost of
302 installing the PRS is certainly superior to the installation of a simple dissipation device, but the
303 significant electricity production that can be obtained from the PRS guarantees a financial benefit
304 that is significantly higher than the installation costs in the case study.
305

306 **Author Contributions:** All authors contributed to the development of this manuscript. Marco Sinagra,
307 Costanza Aricò and Tullio Tucciarelli designed and supervised the hydraulic tests. Pietro Amato designed the
308 PRS turbine and supervised the mechanical components. Michele Fiorino designed electrical control systems
309 and supervised the electrical tests.

310 **Funding:** The experimental plant was funded by "Pressure Management System (PMS) project, grant number
311 no. F/050304/01-03/X32 - Ministero dello Sviluppo Economico D.M. 1 Giugno 2016 Horizon 2020 – PON
312 2014/2020".

313 **Acknowledgments:** We thank the BitControl srl, Layer Electronics srl and Vettorello srl companies, partners in
314 the PMS project, for authorization of scientific use of the experimental results.

315 **Conflicts of Interest:** The authors declare no conflict of interest.

316 References

- 317 1. Perea-Moreno M.A.; Hernandez-Escobedo Q.; Perea-Moreno A.J. Renewable Energy in Urban Areas:
318 Worldwide 2018, *Energies* **2018**, *11*, 577.
- 319 2. Dai J.; Wu S.; Han G.; Weinberg J.; Xie X.; Wu X.; Song X.; Jia B.; Xue W.; Yang Q.; Water-energy nexus: A
320 review of methods and tools for macro-assessment, *Applied Energy* **2018**, *210*, 393-408.
- 321 3. Oikonomou K.; Parvania M. Optimal Coordination of Water Distribution Energy Flexibility With Power
322 Systems Operation, *IEEE Transactions on Smart Grid* **2019**, *10*, 1, 1101-1110.
- 323 4. Baños R.; Reca J.; Martínez J.; Gil C.; Márquez A.L. Resilience Indexes for Water Distribution Network
324 Design: A Performance Analysis Under Demand Uncertainty. *Water Resources Management* **2011**, *25*,
325 2351–2366.
- 326 5. Lotfizadeh H.R.; Barza H.; Abdevalipour M. Controlling the Water Pressure in the Pressure Control.
327 *World Applied Sciences Journal* **2012**, *18* (8): 1088-1094.
- 328 6. Nazif S.; Karamouz M.; Tabesh M.; Moridi A. Pressure Management Model for Urban Water Distribution
329 Networks. *Water Resour Manage* **2010**, *24*, 437– 458.
- 330 7. Prescott S.; Ulanicki B. Improved Control of Pressure Reducing Valves in Water Distribution Networks. *J.*
331 *Hydraul Eng* **2008**, *134*(1), 56–65.
- 332 8. Araujo L.; Ramos H.; Coelho S. Pressure control for leakage minimization in water distribution systems
333 management. *Water Resources Management* **2006**, *20*(1), 133–149.
- 334 9. Carravetta A.; Fecarotta O.; Sinagra M.; Tucciarelli T. Cost-Benefit Analysis for Hydropower Production in
335 Water Distribution Networks by a Pump as Turbine. *J. Water Resour. Plann. Manage.*, **2014**,
336 10.1061/(ASCE)WR.1943-5452.0000384, 04014002.
- 337 10. Sammartano V.; Morreale G.; Sinagra M.; Tucciarelli T. Numerical and experimental investigation of a
338 cross-flow water turbine. *Journal of Hydraulic Research*, **2016**, *55*:5, pages 686-694.
- 339 11. Coelho B., Andrade-Campos A., Energy Recovery in Water Networks: Numerical Decision Support Tool
340 for Optimal Site and Selection of Micro Turbines, *Journal of Water Resources Planning and Management*
341 **2018**, Vol. 144, Issue 3 (March 2018).
- 342 12. Khosrowpanah, S., Albertson, M., Fiuzat, A. Historical overview of Cross-Flow turbine. *Int Water Power*
343 *Dam Constr.* **1984**, 38–43.
- 344 13. Sammartano, V., Aricò, C., Sinagra, M., Tucciarelli, T. Cross-Flow Turbine Design for Energy Production
345 and Discharge Regulation. *J. Hydraul. Eng.* **2014**, 10.1061/(ASCE)HY.1943-7900.0000977, 04014083.
- 346 14. Sinagra, M., Sammartano, V., Aricò, C., Collura, A. Experimental and Numerical Analysis of a Cross-Flow
347 Turbine. *J. Hydraul. Eng.* **2015**, 10.1061/(ASCE)HY.1943-7900.0001061, 04015040
- 348 15. Chen J.; Yang H.X.; Liu C.P.; Lau C.H.; Lo M. A novel vertical axis water turbine for power generation
349 from water pipelines. *Energy* **2013**, *54*, 184– 193
- 350 16. Sinagra M.; Sammartano V.; Aricò C.; Collura A. Experimental and Numerical Analysis of a Cross-Flow
351 Turbine. *Journal of Hydraulic Engineering*, **2016**, 142 - 1 (January 2016).
- 352 17. Carravetta A.; Del Giudice G.; Fecarotta O.; Ramos H. Pump as Turbine (PAT) Design in Water
353 Distribution Network by System Effectiveness. *Water*, **2013**, *5*(3), 1211-1225.
- 354 18. Yang S.; Derakhshan S.; Kong F. Theoretical, numerical and experimental prediction of pump as turbine
355 performance. *Renewable Energy*, **2012**, 507-513
- 356 19. Carravetta A.; Del Giudice G.; Fecarotta O.; Ramos H. Energy Production in Water Distribution Networks:
357 A PAT Design Strategy. *Water Resources Management*, **2012**, *26*,13, 3947–3959.
- 358 20. Carravetta A.; Del Giudice G.; Fecarotta O.; Ramos H.M. PAT Design Strategy for Energy Recovery in
359 Water Distribution Networks by Electrical Regulation. *Energies*, **2013**, *6*(1), 411-424.

- 360 21. Fontana N.; Giugni M.; Glielmo L.; Marini G.; Zollo R. Hydraulic and Electric Regulation of a Prototype for
361 Real-Time Control of Pressure and Hydropower Generation in a Water Distribution Network. *Journal of*
362 *Water Resources Planning and Management*, **2018**, 144 (11).
- 363 22. Sammartano V.; Filianoti P.; Sinagra M.; Tucciarelli T.; Scelba G.; Morreale G. Coupled hydraulic and
364 electronic regulation of cross-flow turbines in hydraulic plants. *Journal of Hydraulic Engineering*, **2017**,
365 143 (1), art. no. 04016071.
- 366 23. Fecarotta O.; Aricò C.; Carravetta A.; Martino R.; Ramos H. M. Hydropower Potential in Water
367 Distribution Networks: Pressure Control by PATs, *Water Resources Management*, **2015**, 29, 3, 699–714.
- 368 24. Balacco, G., Binetti, M., Caporaletti, V. et al. *Int J Energy Environ Eng*, **2018**, 9: 435
- 369 25. Sinagra M., Sammartano V., Morreale, G., Tucciarelli T. A new device for pressure control and energy
370 recovery in water distribution networks. *Water*, 2017, 9 (5).
- 371 26. Sammartano V.; Sinagra M.; Filianoti P.; Tucciarelli T. A Banki–Michell turbine for in-line water supply
372 systems, *Journal of Hydraulic Research*, 2017, 55(5), 686-694.
- 373 27. Sinagra M.; Aricò C.; Tucciarelli T.; Morreale G. Experimental and numerical analysis of a backpressure
374 Banki inline turbine for pressure regulation and energy production. *Renewable energy*. Under review.
- 375 28. Sammartano, V., Aricò, C., Carravetta, A., Fecarotta, O., & Tucciarelli, T. Banki-Michell optimal design by
376 computational fluid dynamics testing and hydrodynamic analysis. *Energies*, **2013**, 6(5), 2362–2385.